

# Allele-Specific Prevention of Nonsense-Mediated Decay in Cystic Fibrosis Using Homology-Independent Genome Editing

Steven Erwood,<sup>1,2,6</sup> Onofrio Laselva,<sup>3,4,6</sup> Teija M.I. Bily,<sup>1</sup> Reid A. Brewer,<sup>1</sup> Alexandra H. Rutherford,<sup>1</sup> Christine E. Bear,<sup>3,4,5</sup> and Evgueni A. Ivakine<sup>1,4</sup>

<sup>1</sup>Program in Genetics and Genome Biology, The Hospital for Sick Children Research Institute, Toronto, ON, Canada; <sup>2</sup>Department of Molecular Genetics, University of Toronto, Toronto, ON, Canada; <sup>3</sup>Program in Molecular Medicine, The Hospital for Sick Children Research Institute, Toronto, ON, Canada; <sup>4</sup>Department of Physiology, University of Toronto, Toronto, ON, Canada; <sup>5</sup>Department of Biochemistry, University of Toronto, Toronto, ON, Canada

**Nonsense-mediated decay (NMD) is a major pathogenic mechanism underlying a diversity of genetic disorders. Nonsense variants tend to lead to more severe disease phenotypes and are often difficult targets for small molecule therapeutic development as a result of insufficient protein production. The treatment of cystic fibrosis (CF), an autosomal recessive disease caused by mutations in the *CFTR* gene, exemplifies the challenge of therapeutically addressing nonsense mutations in human disease. Therapeutic development in CF has led to multiple, highly successful protein modulatory interventions, yet no targeted therapies have been approved for nonsense mutations. Here, we have designed a CRISPR-Cas9-based strategy for the targeted prevention of NMD of *CFTR* transcripts containing the second most common nonsense variant listed in CFTR2, W1282X. By introducing a deletion of the downstream genic region following the premature stop codon, we demonstrate significantly increased protein expression of this mutant variant. Notably, in combination with protein modulators, genome editing significantly increases the potentiated channel activity of W1282X-*CFTR* in human bronchial epithelial cells. Furthermore, we show how the outlined approach can be modified to permit allele-specific editing. The described approach can be extended to other late-occurring nonsense mutations in the *CFTR* gene or applied as a generalized approach for gene-specific prevention of NMD in disorders where a truncated protein product retains full or partial functionality.**

## INTRODUCTION

Nonsense mutations account for an estimated 11% of the variants underlying inherited disease.<sup>1</sup> Though the molecular consequences of a nonsense mutation are varied,<sup>2</sup> the predominant outcome of this type of mutation is degradation of the resulting mRNA transcript through a process called nonsense-mediated decay (NMD). Often, this degradation results in the complete absence of protein or residual production of a truncated protein product. If NMD is prevented or escaped, these truncated protein products may result in dominant-negative or gain-of-function phenotypes.<sup>2</sup> For an accumulating number of disor-

ders, however, it has been demonstrated that the prevention of NMD can attenuate disease phenotypes.<sup>3–5</sup>

Cystic fibrosis (CF; MIM: 219700) is an autosomal recessive disorder caused by mutations in the CF transmembrane conductance regulator (*CFTR*) gene. The *CFTR* protein is an ion channel that mediates chloride and bicarbonate transport in the epithelial cells of multiple organs including the lungs, pancreas, and intestine.<sup>6–8</sup> To date, more than 300 CF-causing mutations have been identified (<http://www.genet.sickkids.on.ca/>; <https://cftr2.org/>). The most common mutation, the deletion of phenylalanine at position 508 (F508del-*CFTR*), induces misfolding of the protein that results in its retention within the endoplasmic reticulum and subsequent degradation by proteasomal pathways. Recently, the combination of two correctors, Tezacaftor (VX-661) and Elexacaftor (VX-445), alongside a channel function potentiator called Ivacaftor (VX-770) has been approved by the FDA as TRIKAFTA for patients with one or two F508del-*CFTR* alleles.<sup>9–12</sup> Despite the promising reports that treatment with TRIKAFTA is associated with meaningful improvement in lung function and respiratory-related quality life, no modulator therapies are clinically available for individuals with nonsense mutations in *CFTR*. The second most common nonsense mutation in CF, W1282X-*CFTR* (NC\_000007.14:g.117642566G > A), is subject to nonsense-mediated mRNA decay and results in residual expression of a truncated protein product.<sup>13,14</sup> While it has been shown that *CFTR* modulators are effective at rescuing the functional expression of W1282X-*CFTR* in systems of heterologous overexpression, this has not been universally successful in primary cultures of airway epithelia.<sup>15</sup> Recently it has been demonstrated that a combination of *CFTR* correctors and a potentiator, alongside a small molecule that inhibits NMD, can rescue

Received 15 April 2020; accepted 7 May 2020;  
<https://doi.org/10.1016/j.omtm.2020.05.002>.

<sup>6</sup>These authors contributed equally to this work.

**Correspondence:** Evgueni A. Ivakine, Program in Genetics and Genome Biology, The Hospital for Sick Children Research Institute, Toronto, ON, Canada.

**E-mail:** [zhenya.ivakine@sickkids.ca](mailto:zhenya.ivakine@sickkids.ca)



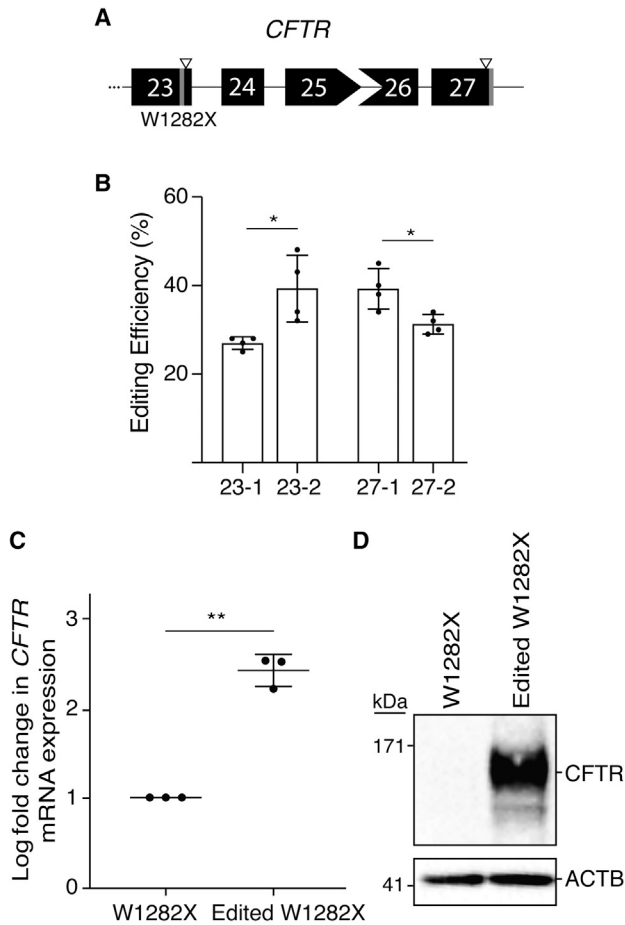


**Figure 1. Genome Editing Restores Expression of W1282X-CFTR in Human Bronchial Epithelial Cells**

(A) Schematic illustrates the editing strategy. The premature and native stop codons are indicated by a gray line. The CRISPR-Cas9 cleavage sites are indicated by open arrowheads. Exon shape indicates open reading frame. (B) Editing efficiency of guides targeting exon 23 and exon 27 were evaluated in HEK293T cells. The most efficient guides targeting each exon were selected for subsequent experiments,  $n = 3$  biological replicates,  $p = 0.0452$  and  $p = 0.0309$ . Data are plotted as the mean with error bars representing the standard deviation. (C) Expression of CFTR mRNA was measured by quantitative real-time PCR in a bulk edited cell population of W1282X-CFTR HBE cells compared to parental controls,  $n = 3$  biological replicates,  $p = 0.0047$ . Data are plotted as the mean with error bars representing the standard deviation. (D) Expression of CFTR protein was measured by western blot with ACTB used as a loading control.

the functional expression of W1282X-CFTR in patient-derived nasal epithelial cells.<sup>16</sup>

Through its demonstrated role in maintaining proper gene expression,<sup>17,18</sup> NMD underlies a diversity of fundamental biological processes, ranging from the maturation of the immune system to the maintenance of telomeres.<sup>19–22</sup> The importance of NMD is highlighted through its broad phylogenetic conservation.<sup>23</sup> Accordingly, strategies that rely on global inhibition of NMD may be coupled

with a variety of off-target effects with far-reaching phenotypic consequences.

Presently, gene therapy is being actively explored for the treatment of CF, particularly for those carrying nonsense mutations. Although this approach has shown promising preliminary results in various model systems,<sup>24–28</sup> insufficient transgene delivery and expression—largely attributed to loss over cell divisions—have proven to be a challenge in the clinical translation of gene therapy for CF.<sup>29,30</sup> Targetable nucleases, most notably the CRISPR-Cas9 system, have become an attractive alternative to traditional gene therapy approaches. The precise correction of disease-causing mutations, however, remains a significant challenge for genome editing technologies. Although several groups have demonstrated mutation correction and restored expression of wild-type (WT) CFTR,<sup>31–33</sup> their reliance on the relatively inefficient homology-directed repair (HDR) pathway can be prohibitive in terms of the clinical translation of these strategies. Consequently, many therapeutic applications of genome editing have focused on strategies involving non-homologous end joining (NHEJ),<sup>34,35</sup> which tends to occur at a much higher frequency than homology-directed repair.<sup>36</sup>

In the present study, we describe a CRISPR-Cas9-based genome editing strategy that harnesses NHEJ to prevent NMD in a gene-specific manner. Using a dual-guide approach, we generated an approximately 24-kilobase deletion spanning from exon 23 to exon 27 of the *CFTR* locus, encompassing the downstream genic region following W1282X-CFTR. While not fully understood, NMD tends to occur in a splicing-dependent manner, triggered by exon-junction complexes remaining downstream of a prematurely-terminated ribosome.<sup>37</sup> We hypothesized that this editing strategy would eliminate the formation of exon-junction complexes following the premature stop codon and thus prevent NMD of the edited transcript.<sup>38</sup> Using human bronchial epithelial (HBE) cells that are homozygous for the W1282X mutation, we show that the desired deletion can be achieved with high efficiency and that editing results in the restoration of CFTR expression at both the mRNA and protein level. Further, we show that the resulting protein product can be successfully modulated with clinically approved CFTR modulators. To account for the heterogeneity in genotypes across patients with CF, we refined our editing strategy to permit allele-specific editing. Our data demonstrate a novel use case for CRISPR-Cas9 genome editing in gene-specific prevention of NMD, which could be further applied to other genetic diseases caused by nonsense mutations.

## RESULTS

### CRISPR-Cas9-Mediated Genome Editing Allows for Genomic Truncation of CFTR

Using CRISPR-Cas9, a genomic deletion can be efficiently generated by simultaneously targeting the region of interest using two flanking guide RNAs.<sup>39–42</sup> We hypothesized that removal of the downstream genic region following the mutation site would prevent NMD upon subsequent transcription, thereby stabilizing CFTR expression (Figure 1A). We designed four guide RNAs—two targeting exon 23

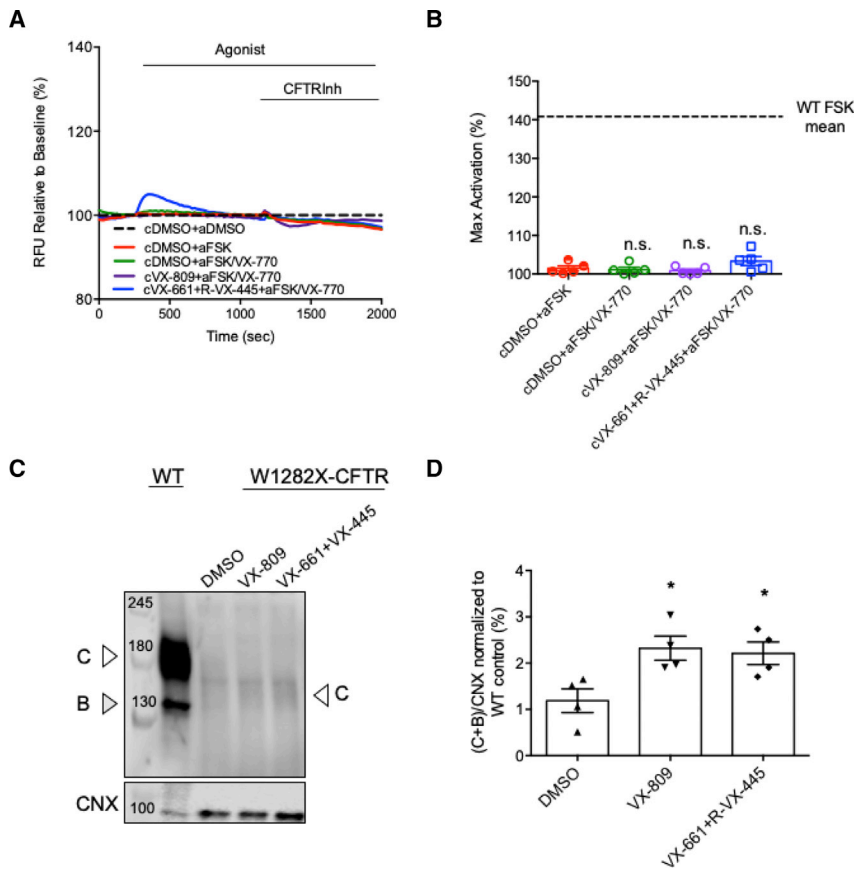


**Figure 2. W1282X-CFTR Human Bronchial Epithelial Cells Show No Functional Rescue after Treatment with the Novel Approved F508del-CFTR Modulator Therapy**

(A) Representative trace of W1282X-CFTR dependent chloride efflux using the FLIPR assay in HBE cells pretreated with DMSO (cDMSO), 3  $\mu$ M VX-809 (cVX-809), 10  $\mu$ M VX-661+ 3  $\mu$ M [R]-VX-445 (cVX-661+R-VX-445) for 24 h at 37°C. Following baseline measurement, 10  $\mu$ M FSK  $\pm$  1  $\mu$ M VX-770 were added to activate and potentiate the channel activity and the CFTR inhibitor (CFTRinh-172, 10  $\mu$ M) was added to inactivate CFTR. (B) Bar graphs show the mean ( $\pm$ SEM) of peak CFTR-mediated depolarization response after stimulation by FSK  $\pm$  VX-770 (aFSK or aFSK/VX-770; n = 5 biological replicates with each symbol being a mean 4 technical replicates). (C) Representative blot of WT-CFTR and CRISPR-Cas9-edited W1282X-CFTR HBE cells after 24 h treatment with CFTR modulators. C, mature complex-glycosylated; B, immature core-glycosylated; CNX, loading control, calnexin. (D) Bars represent the mean ( $\pm$ SEM) of total CFTR (C+B)/CNX normalized to WT control (%; n = 4 biological replicate; \*p < 0.05).

following the premature stop codon, and two targeting exon 27, the final exon of CFTR. These guides were designed and selected to minimize potential off-target editing using the CHOPCHOP webtool.<sup>43</sup> We transfected each of these guides individually alongside *Streptococcus pyogenes* Cas9 (SpCas9) into HEK293T cells to evaluate editing efficiency. We found that editing efficiencies ranging from 25%–48% (Figure 1B). To introduce the desired deletion, we paired the guides with highest editing efficiency from the two targeted loci. When transfected individually alongside SpCas9 into W1282X-HBE cells, these guides exhibited similar editing activities to those found in the HEK293T experiments (Figure S1A). These guides were co-transfected into an immortalized human bronchial epithelial cell line that was previously gene edited using CRISPR-Cas9 to harbor the W1282X-CFTR variant in homozygosity.<sup>44</sup> Using a polymerase chain reaction (PCR)-based assay, we identified a product corresponding to a deletion junction formed across the two cleavage sites in the genomic DNA of the edited cell population (Figure S1B).

#### Genome Editing Improves Expression of W1282X-CFTR Protein and mRNA in Human Bronchial Epithelial Cells

After establishing that the desired deletion was achievable, we sought to evaluate how editing impacted W1282X CFTR expression. In a heterogeneous population of edited cells, we found a  $2.4 \pm 0.18$ -fold increase in *CFTR* mRNA expression compared to unedited

controls (Figure 1C). Correspondingly, a truncated mRNA transcript was present in the cDNA of the edited W1282X-CFTR HBE cell population that was absent in unedited W1282X-CFTR control HBE cells (Figure S1C). In addition to an increase in *CFTR* mRNA expression, edited cells exhibited modest expression of the truncated CFTR protein, which was absent in unedited cells (Figure 1D). Together, these data demonstrate that the genomic truncation of the W1282X-CFTR variant can successfully prevent NMD.

#### Genome-Edited Human Bronchial Epithelial Cells Produce Functional CFTR Protein after Pharmacological Rescue

Previous studies suggested that small molecule correctors and potentiators were partially effective in rescuing the channel activity of W1282X-CFTR.<sup>15,16,45,46</sup> We sought to determine whether the recently approved drug combination, TRIKAFTA, which targets the F508del mutation, is able to rescue W1282X-CFTR channel activity in homozygous mutant human bronchial epithelial (HBE) cells.<sup>16,44</sup> As expected, prior to editing there was no residual forskolin (FSK) activated, i.e., cyclic adenosine monophosphate (AMP)-mediated channel activity conferred by W1282X-CFTR in HBE cells (Figure 2A and 2B). Further, there was no functional rescue of potentiated channel function following pre-treatment with the first-generation corrector, VX-809, or the second-generation corrector combination, VX-661 and VX-445, in the current studies (Figures 2A and 2B). Immunoblotting studies confirmed that W1282X-CFTR protein was truncated and at only 1% of the abundance measured for WT-CFTR in HBE cells (Figures 2C and 2D). There was only a modest increase in the abundance of the truncated protein in the presence of the correctors.

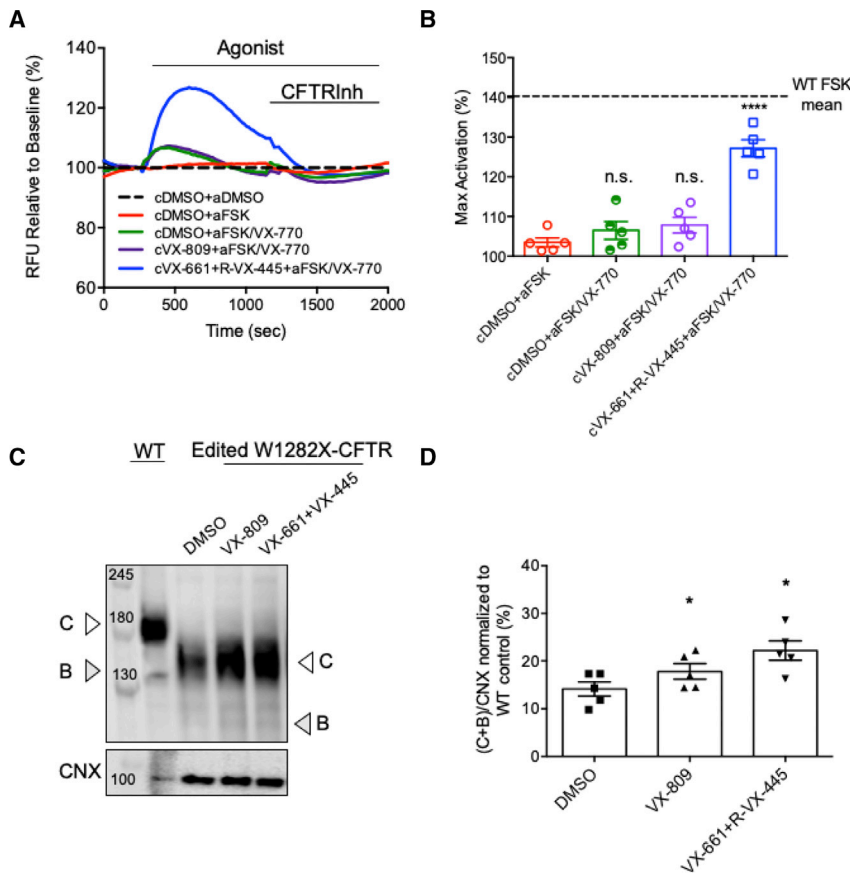


**Figure 3. W1282X-CFTR Is Rescued by Genome Editing and a Second-Generation Corrector Combination**

(A) Representative trace of W1282X-CFTR gene-edited dependent chloride efflux using the FLIPR assay in HBE cells pretreated with DMSO (cDMSO), 3  $\mu$ M VX-809 (cVX-809), 10  $\mu$ M VX-661+ 3  $\mu$ M [R]-VX-445 (cVX-661+R-VX-445) for 24 h at 37°C. Following baseline measurement, 10  $\mu$ M FSK  $\pm$  1  $\mu$ M VX-770 (aFSK or aFSK/VX-770) were acutely added. CFTR inhibitor (CFTRinh-172, 10  $\mu$ M) was added to inactivate CFTR. (B) Bar graphs show the mean ( $\pm$ SEM) of peak CFTR-mediated depolarization response after stimulation by FSK  $\pm$  VX-770 (n = 5 biological replicates with each symbol being the mean of 4 technical replicates). (C) Representative blot of WT-CFTR and W1282X-CFTR gene-edited HBE cells after 24 h treatment with CFTR modulators. C, mature complex-glycosylated; B, immature core-glycosylated; CNX, loading control, calnexin. (D) Bars represent the mean ( $\pm$ SEM) of total CFTR (C+B)/CNX normalized to WT control (%; n = 5 biological replicates; \*p < 0.05, \*\*\*\*p < 0.0001).

Since deleting the downstream genic region increased protein expression of truncated W1282X-CFTR (Figure 1D), we asked whether modulators could rescue functional expression in the gene-edited HBE cells. While there was no functional response to potentiation with VX-770 alone or with VX-809 pre-treatment with acute addition of VX-770 (Figures 3A and 3B), we did see a significant rescue of potentiated W1282X-CFTR function (70% of the mean forskolin in WT-CFTR HBE cells) after pre-treatment with the novel modulators VX-661 and VX-445. Gene-edited W1282X-CFTR HBE cells demonstrated up to 70% of the mean forskolin response observed in WT-CFTR HBE cells. As shown in Figures 3C and 3D, we achieved approximately 20% of WT-CFTR protein abundance under the best rescue conditions. Altogether, these findings support the use of this editing strategy to generate a partially functional, truncated CFTR mutant that has the potential for channel activity in the presence of channel function modulators.

**Allele-Specific Genome Editing of W1282X-CFTR**

Most patients harbor the W1282X-CFTR mutation in compound heterozygosity. To account for this, we aimed to modify our strategy to minimize targeting of the other mutant allele. It has been demonstrated that a mismatch in the seed sequence of a guide RNA—the 10–12 nucleotides immediately upstream of the protospacer adjacent motif (PAM) sequence—can significantly reduce or even abolish the

editing activity of CRISPR-Cas9.<sup>47–49</sup> We strategically designed a guide RNA where the first PAM-proximal nucleotide of the sequence is complementary to the adenine nucleotide underlying the W1282X-CFTR variant (Figure 4A). To assess the precision of this guide RNA, we transfected it in a vector co-expressing SpCas9 into both WT- and W1282X-CFTR HBE cells. We found a significant bias toward alleles harboring the W1282X-CFTR variant compared to alleles that are WT at this locus, with average editing efficiency of 30.25%  $\pm$  1.26% and 0%, respectively (Figure 4B). As a control, we designed a reciprocal guide RNA, where the first PAM-proximal nucleotide is complementary to the WT sequence, and found corresponding allelic discrimination with average editing efficiency of 31%  $\pm$  1.41% in the context of the mutant allele and 83.5%  $\pm$  6.16% in the context of the WT allele (Figure S2).

To generate a deletion, we paired the W1282X-CFTR-specific guide RNA with a guide RNA targeting 108 bases downstream of the native stop codon in the 3' UTR of *CFTR* (Figure 4C). While this guide RNA is indiscriminate of alleles, we hypothesized that any potential indels formed on the non-targeted allele would have a negligible effect on CFTR expression or function, due to being placed within a non-coding region. To test this, we transfected this guide RNA in a vector co-expressing SpCas9 into WT-CFTR HBE cells and evaluated CFTR protein expression following editing. We found that CFTR expression remained stable, which indicates that this guide is likely benign (Figure S3A). In addition, we found similar results when evaluating CFTR protein expression of WT-CFTR HBE cells after delivery of the W1282X-CFTR targeting guide RNA both individually and combined with the guide targeting the 3' UTR, further supporting the allele-specificity of the designed approach (Figure S3A). In addition

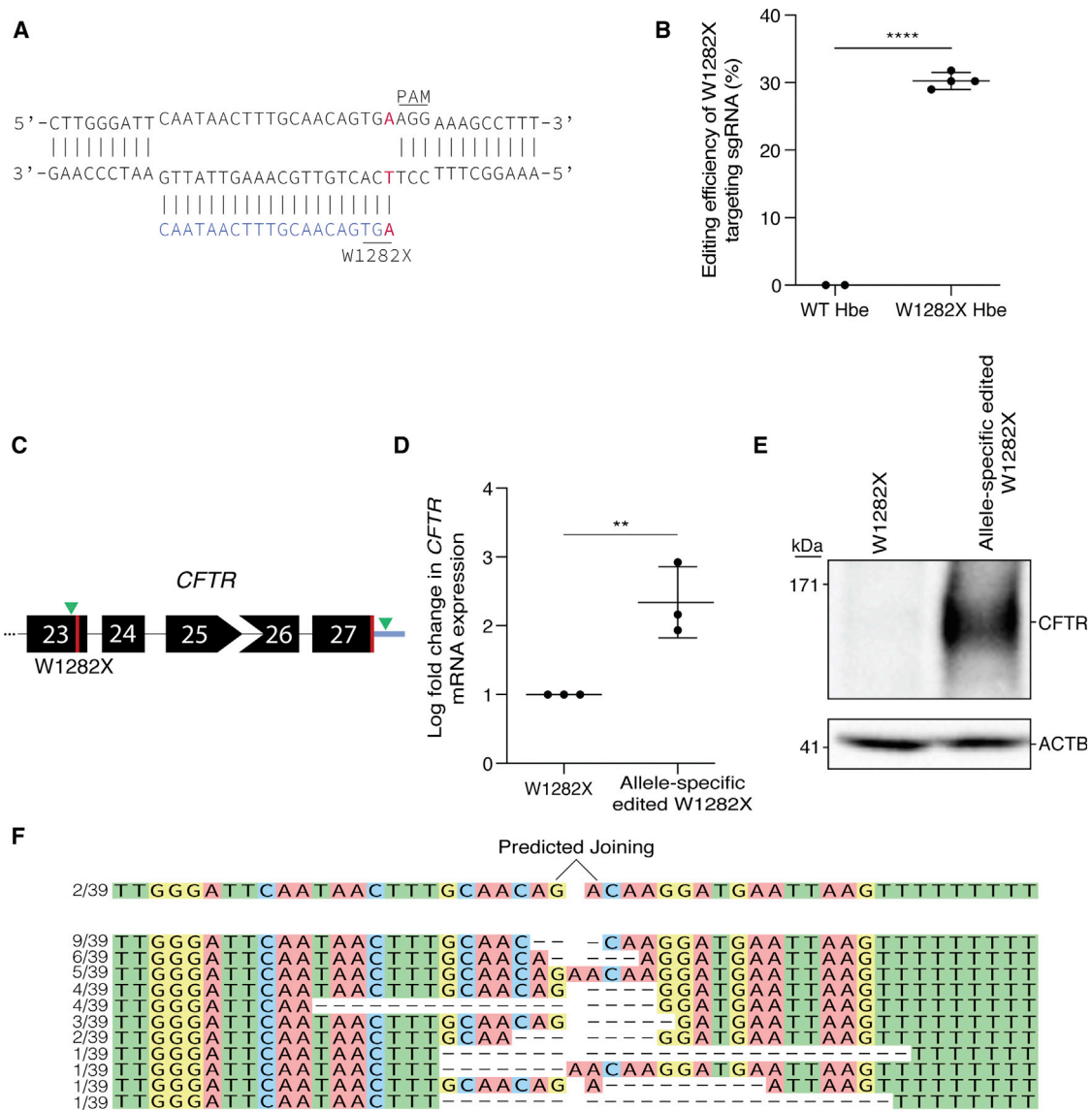


**Figure 4. Allele-Specific Editing Restores Expression of Truncated CFTR**

(A) Schematic illustrating the allele-specific targeting of the W1282X-CFTR locus. The first PAM-proximal nucleotide is specific to the point mutation underlying W1282X-CFTR. (B) Editing efficiency of the W1282X-CFTR targeting guide was tested in WT and homozygous W1282X-CFTR HBE cells,  $n = 3$ ,  $p < 0.0001$ . Data are plotted as the mean with error bars representing the standard deviation. (C) Schematic illustrating the position of the CRISPR-Cas9 cleavage sites for allele specific editing. Cleavage sites are indicated by green arrows, stop codons are indicated by red lines, and the 3' UTR is indicated in light blue. Exon shape indicates open reading frame. (D) Expression of CFTR mRNA was measured by quantitative real-time PCR in bulk-edited W1282X-HBE cell populations compared to parental controls,  $n = 3$ ,  $p = 0.0126$ . Data are plotted as the mean with error bars representing the standard deviation. (E) CFTR protein expression was measured by western blot with ACTB as a loading control in parental controls and a bulk population of allele-specific edited W1282X-HBE cells. (F) An allele table illustrating the varied editing outcomes resulting from allele-specific editing. The predicted joining is represented on top and all other outcomes below. Dashes indicate deleted bases.

to targeting outside of the coding region of *CFTR*, we selected the 3' UTR targeting guide as it introduces a novel termination codon 15 bases downstream of the predicted deletion junction. This was necessary as the allele-specific guide RNA generates a double-stranded break immediately before the premature stop codon such that when combined with a guide RNA that targets beyond the coding region of the gene, the result is a removal of both the premature and native

stop codon found in the W1282X-CFTR allele. Accordingly, the predicted result of our editing is the production of CFTR protein that is WT up to the 1,281<sup>st</sup> residue, followed by a novel sequence of four amino acids and a stop codon (Figure 4F).

We co-delivered these two guide RNAs alongside SpCas9 into W1282X-CFTR HBE cells to assess their impact on CFTR expression.

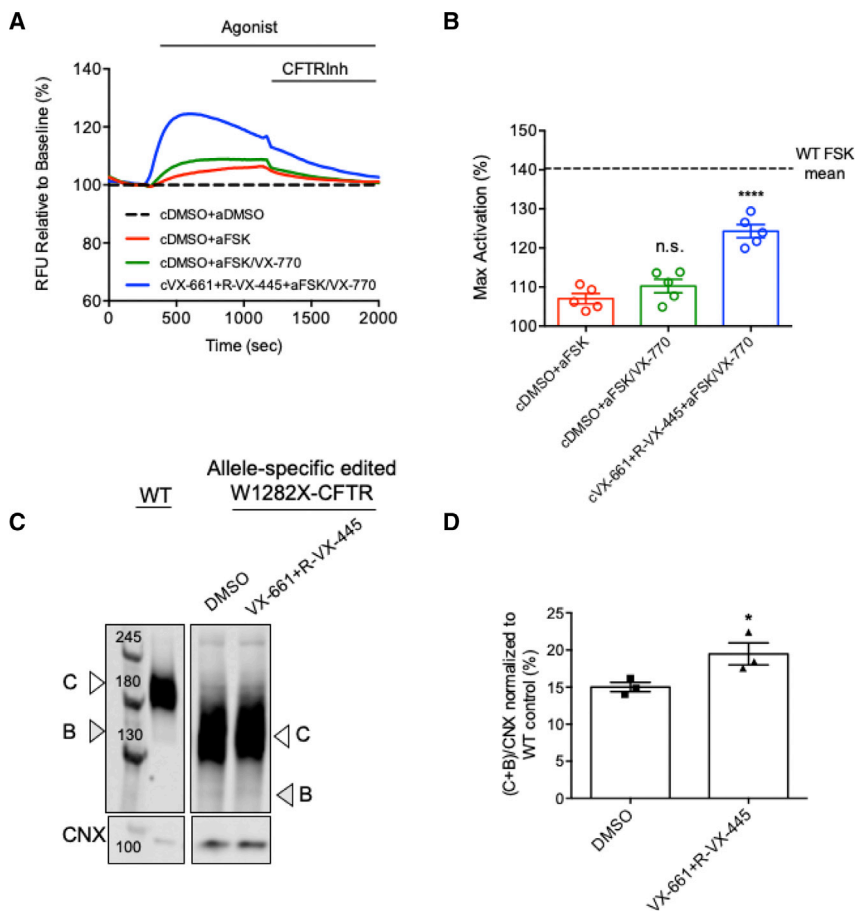


**Figure 5. Functional Expression of Truncated CFTR Is Improved by Allele-Specific Genome Editing and a Second-Generation Corrector Combination**

(A) Representative trace of W1282X-CFTR allele-specific gene-edited dependent chloride efflux using the FLIPR assay in HBE cells pretreated with DMSO (cDMSO), 10  $\mu$ M VX-661+ 3  $\mu$ M [R]-VX-445 (cVX-661+R-VX-445) for 24 h at 37°C. Following baseline measurement, 10  $\mu$ M FSK  $\pm$  1  $\mu$ M VX-770 (aFSK or aFSK/VX-770) was acutely added. CFTR inhibitor (CFTRinh-172, 10  $\mu$ M) was added to inactivate CFTR. (B) Bar graphs show the mean ( $\pm$ SEM) of peak CFTR-mediated depolarization response after stimulation by FSK  $\pm$  VX-770 (n = 5 biological replicates with each symbol being a mean of 6 technical replicates). (C) Representative blot of WT-CFTR and W1282X-CFTR allele specific gene-edited HBE cells after 24 h of treatment with CFTR modulators. C, mature complex-glycosylated; B, immature core-glycosylated; CNX, loading control, calnexin. (D) Bars represent the mean ( $\pm$ SEM) of total CFTR (C+B)/CNX normalized to WT control (%; n = 3 biological replicates; \*p < 0.05, \*\*\*\*p < 0.0001).

By PCR, we were able to detect the formation of a deletion junction in genomic DNA extracted 72 h post-transfection. Using a three primer PCR assay, we quantified the proportion of DNA containing the desired deletion relative to unedited DNA, finding similar amplification intensity of each product (Figure S4A). The introduction of the intended stop codon requires perfect joining of the two double-stranded breaks. We subcloned the amplified deletion junction and found the predicted editing in only 5% of clones screened (2/39 clones). Instead, we found a heterogeneous population of deletion junctions with indels of varied length. In each of the editing outcomes, however, a novel stop codon was reached within 1–36 amino acids of the 1,281<sup>st</sup> residue, with the majority of editing outcomes (30/39 clones) producing a stop codon within four amino acids.

Next, we analyzed the effect of our editing strategy on CFTR expression at the level of mRNA and protein. We extracted protein and mRNA from both edited (W1282X-CFTR edited) and unedited (W1282X-CFTR) HBE cells, 5 days post-confluence. The expression of CFTR mRNA in a heterogeneous population of edited cells was increased  $2.34 \pm 0.26$ -fold when compared to unedited controls (Figure 4D). Again, we found the expression of a truncated CFTR mRNA product (Figure S4B) and truncated CFTR protein product in the edited W1282X-CFTR cells that was absent in W1282X-

CFTR control cell population. (Figure 4E). Finally, we asked whether the CFTR protein expression rescued by allele-specific editing could be modulated by second-generation modulator compounds similar to our non-specific editing experiments. As shown in Figures 5A and 5B, we measured residual function of the truncated CFTR product after editing in an allele-specific manner that was not further potentiated by VX-770. After the addition of the combination of VX-661 and [R]-VX-445, we observed rescued potentiated channel function (60% of the mean forskolin in WT-CFTR HBE cells) in W1282X-CFTR HBE cells after allele-specific editing. We also found that the corrector modulators enhanced the relative expression of truncated CFTR in allele-specific edited W1282X-CFTR HBE cells (Figures 5C and 5D).

## DISCUSSION

Significant advancements have been made in the therapeutic development for CF, culminating in a wide variety of highly effective small molecule therapies.<sup>11,50,51</sup> These therapies, which have largely focused on the predominant F508del-CFTR variant, are inapplicable to patients harboring nonsense mutations in CFTR. Due to the decay of mRNA transcripts, nonsense mutations in CFTR lead to reduced or absent expression of truncated CFTR protein. Consequently, there is an urgent unmet need for clinical development targeted toward nonsense mutations in CF. For one such nonsense mutation, W1282X-CFTR, it has been demonstrated that if NMD can be prevented, either through heterologous expression or through the pharmacological inhibition of NMD, the truncated protein product can be effectively modulated using existing CFTR modulators.<sup>14,16,52,53</sup>

In our previous experience, the steady-state levels of W1282X protein, endogenously expressed in epithelial cell lines and in primary tissues, are negligible. This reduced expression can be reversed by treatment with nonsense mediated decay inhibitors, pointing to the negative impact of this pathway. Recently, we tested three NMD small molecule inhibitors with different mechanisms of action in W1282X-CFTR HBE cells.<sup>16</sup> We compared the relative efficacy of a SMG-1 kinase inhibitor (SMG1), 5-azacytidine (Vidaza, that acts via the MYC-dependent pathway), and NMD-14 that targets the SMG7 protein and disrupts SMG7-UPF1 interactions. Interestingly, we observed that modulation of NMD by inhibition of SMG-1 protein was the most effective in rescuing the truncated W1282X-CFTR channel function after pre-treatment with CFTR correctors. The clinical utility of such NMD inhibitors, however, is uncertain given the potential for toxic off-target effects. It is well-established that for CFTR, the final domain of this multi-domain protein, is not required for its folding and assembly. Truncation mutants lacking the second nucleotide binding domain are properly processed and trafficked to the surface of cells in heterologous expression systems.<sup>14–16</sup> These truncation mutants, however, do require pharmacological modulators for channel function activation. These observations prompted the development of the therapeutic strategy described in this paper.

We designed a homology-independent genome editing strategy that successfully suppresses NMD of the second most common disease-causing nonsense mutation in CF. The magnitude of functional rescue reported here is similar to what we found previously with the most effective NMD inhibitors.<sup>16</sup> Our approach generates a truncated *CFTR* transcript that escapes NMD and produces a protein product that can be therapeutically modulated with existing small molecule compounds designed for the more common F508del-CFTR variant.

Notably, we demonstrate that the protein product generated is effectively modulated using the drug combination comprising TRIKAFTA.<sup>11,50</sup> This stands as the first demonstration of the potential therapeutic benefit of TRIKAFTA specifically for the W1282X-CFTR variant. In its final iteration, our approach was modified such that targeting was specific to alleles carrying the W1282X-CFTR mutation. This allele-specific approach can be applied to patients who harbor the W1282X-CFTR mutation in heterozygosity while leaving the non-targeted allele intact (i.e., N1303K/W1282X).

Although our results and those of previous publications show that the truncated W1282X-CFTR can reach the cell surface and mediate chloride conductance after treatment with CFTR modulators, the stability of the truncated protein at the apical membrane of epithelia will be compromised. The carboxyl CFTR terminus (<sup>1478</sup>TRL<sup>1480</sup>) is responsible for binding to several PSD-95/Dlg/ZO-1 (PDZ) domain-containing proteins including NHERF-1 (Na<sup>+</sup>/H<sup>+</sup> exchanger regulatory factor isoform 1), NHERF-2, CAP-70 (CFTR-associated protein), and CAL (CFTR associated ligand).<sup>54</sup> It has been demonstrated that overexpression of NHERF1 stabilizes the most common CFTR mutation, F508del, at the apical membrane.<sup>55</sup> Furthermore,

the CFTR corrector VX-809 stabilizes F508del-CFTR at the cell surface by increasing the interaction between F508del-CFTR and NHERF1.<sup>56–58</sup> As recently suggested by Lukacs and colleagues, however, steady-state abundance of mutant CFTR that lacks its carboxy-terminal PDZ motif on the apical membrane may be maintained, at least in part, by efficient transcytosis from the basolateral membrane. This group has shown that mutant CFTR lacking six residues from its carboxy terminus exhibits transcytosis to the apical membrane and this does not require PDZ-dependent interactions.<sup>59</sup>

Here, we chose to truncate the CFTR gene at the site of the premature termination codon (PTC), with the truncation encompassing the entire downstream genic region. It has been documented, however, that the size of deletion is highly correlated with the efficiency of deletion.<sup>60</sup> Although we show that the editing efficiency achieved is sufficient for significant rescue of expression, there are optimizations to the editing strategy that could further increase deletion efficiency and that are applicable to both W1282X-CFTR and other pathogenic PTCs. For example, sensitivity to NMD is correlated with distance from the PTC to the nearest downstream exon junction complex, with insensitivity being documented at distances greater than 50 nucleotides.<sup>61–65</sup> Accordingly, a deletion that joins the PTC-containing exon to the next following exon greater than 50 nucleotides in length could reduce or eliminate NMD. If applied to W1282X-CFTR, this would require removing 10 kilobases, which may occur at a higher frequency than the presented 24-kilobase deletion. This approach, however, would need to be validated on a case-by-case basis, as multiple exceptions to the 50-nucleotide NMD boundary have been documented,<sup>66–69</sup> and there may be a tradeoff between deletion efficiency and residual NMD activity.<sup>70</sup> CRISPR-Cas9-mediated exon skipping<sup>71</sup> is another viable homology-independent genome-editing approach that could be applied to the W1282X-CFTR variant, as exclusion of the mutation-containing exon preserves the proper reading frame. The stability and drug responsiveness of the resulting protein product, however, would need to be verified, though it is likely that this protein product could be similarly modulated with some combination of existing therapeutic compounds.

To further translate this strategy, varied optimizations will be required with respect to delivery. The most common vehicle being explored for the delivery of genome-editing components is the adeno-associated viral (AAV) vector.<sup>72</sup> The large size of SpCas9, however, poses a challenge given the limited packaging capacity of AAV vectors.<sup>73</sup> This has recently been addressed by the development of various split-SpCas9 systems that allow for packaging of the enzyme across multiple AAV particles for *in vivo* reconstitution.<sup>74–76</sup> Alternatively, the editing strategy could be translated to one of the more compact Cas9 orthologs, such as *Staphylococcus aureus*, *Campylobacter jejuni*, or *Streptococcus thermophilus*, all of which have been demonstrated *in vivo* using AAV-based delivery.<sup>77–79</sup>

While demonstrated with the W1282X-CFTR variant, this strategy could be extended to any nonsense or frameshift mutation occurring downstream of the 1,281<sup>st</sup> residue, such as Y1307X-, Q1412X-, or

S1455X-CFTR. It is possible that a larger C-terminal truncation could be similarly modulated, further expanding the number of CFTR nonsense mutations targetable using this approach. Further, our strategy could serve as a generalized approach to the prevention of NMD in genetic diseases where a truncated protein product of the causative gene retains full or partial functionality.<sup>3,5,80</sup>

## MATERIALS AND METHODS

### Cell Culture and Transfection

HEK293T cells were purchased from ATCC and were cultured in Dulbecco's modified Eagle's medium (Wisent) supplemented with 10% fetal bovine serum and 1% penicillin/streptomycin (Pen-Strep; GIBCO). 16HBE cells (a generous gift from Dr. D.C. Gruenert, University of California, San Francisco, CA, USA) and CFF-16HBEge W1282X-CFTR cells (from Cystic Fibrosis Foundation) were cultured in Eagle's minimum essential medium (Wisent) supplemented with 10% fetal bovine serum and 1% Pen-Strep (GIBCO). We seeded 500,000 cells for transfection in 2 mL of media in six-well plates using Lipofectamine 3000 (Thermo Fisher Scientific). Cells were transfected with 3,000 ng of a Cas9 and guide RNA co-expression vector, pSpCas9(BB)-2A-Puro (PX459) V2.0, which was a gift from Feng Zhang (Addgene plasmid #62988). To enrich for transfected cells, we subject 24 h post-transfection cells to 0.9 µg/mL or 2 µg/mL of puromycin, for HBE cells and HEK293T cells, respectively, for 72 h.

### Compound Description

VX-809, VX-661, and VX-770 were provided by Selleck Chemicals; [R]-VX-445 (N-(1,3-dimethylpyrazol-4-yl)sulfonyl-6-[3-(3,3,3-trifluoro-2,2-dimethyl-propoxy)pyrazol-1-yl]-2-[(4R)-2,2,4-trimethylpyrrolidin-1-yl]pyridine-3-carboxamide) and [S]-VX-445 (N-(1,3-dimethylpyrazol-4-yl)sulfonyl-6-[3-(3,3,3-trifluoro-2,2-dimethyl-propoxy)pyrazol-1-yl]-2-[(4S)-2,2,4-trimethylpyrrolidin-1-yl]pyridine-3-carboxamide) were provided by MedChemExpress. For these studies we employed the R enantiomer of VX-445 provided by MED-CHEMEXPRESS. Comparative studies of the enantiomers showed similar activity using the fluorescence plate reader (FLIPR) assay in W1282X-CFTR HBE cells (maximal activation: R enantiomer  $103.4 \pm 1.144$  and S enantiomer  $105 \pm 0.7141$ ).

### Genomic DNA Isolation and PCR

Genomic DNA was isolated using the DNeasy Blood and Tissue Kit (QIAGEN) according to the manufacturer's protocol. PCR was performed using DreamTaq Polymerase (Thermo Fisher Scientific) according to the manufacturer's protocol.

### Estimation of Genome Editing

PCR amplification from the genomic DNA of a bulk population of edited cells centered on the predicted editing site was performed. These amplicons were PCR purified using QIAquick PCR Purification Kit following the manufacturer's protocol (QIAGEN) and Sanger sequenced using an internal primer. To test guide efficiency, we used the Sanger sequencing files from unedited and edited cells as an input into the online sequence trace decomposition software Synthego Performance Analysis, ICE Analysis (2019, v2.0. Synthego).<sup>81</sup> To assess

the editing outcomes found after allele-specific editing, we performed a PCR to amplify the deletion junction formed between the two double-stranded break points. This amplicon was then purified and subcloned using the pGEM-T Easy Vector System (Promega). The cloned plasmid was extracted from 40 unique clones and sequenced with a primer complementary to the vector backbone. To assess editing activity in the WT HBE cell populations (represented in Figure S3), we digested PCR products using the T7 Endonuclease I Enzyme (New England Biolabs) following the manufacturer's instructions. This was necessary as sequencing-based methods were infeasible for the 3' UTR-targeted region due to long adenine tracts interfering with Sanger sequencing. To estimate frequency of the deletion product in genomic DNA from a bulk edited population, we used a three-primer PCR strategy. Primer pairs were designed such that the combination of three primers would result in amplification of both unedited DNA and DNA spanning a deletion junction. Each primer pair utilizes the same forward primer and distinct amplification is derived from the reverse primer design. Choice of reverse primers was based on maintaining similar DNA amplicon size between targets and matching melting temperatures to the universal forward primer.

### CFTR Channel Function in CFF-16HBEge W1282X-CFTR Cells

16HBE14o- cells, previously genome-edited to produce the homozygous CFF-16HBEge W1282X-CFTR cell line, were obtained from the Cystic Fibrosis Foundation.<sup>44</sup> Cells were grown at 37°C for 5 days post-confluence, submerged on 96-well black-well, clear-bottom culture plates (Costar) in EMEM media (Wisent BioProducts) with 10% fetal bovine serum (Wisent BioProducts) and 1% Pen-Strep (Wisent BioProducts). 24 h before the assay, cells were treated with DMSO, 3 µM VX-809 (Selleck Chemicals), and 10 µM VX-661 (Selleck Chemicals) + [R]-VX-445 (MedChemExpress). Cells were then loaded with blue, membrane potential dye dissolved in chloride-free buffer (150 mM NMDG-gluconate, 3 mM potassium gluconate, 10 mM HEPES, pH 7.30, 300 mOsm) for 30 min. The plate was then read in a FLIPR Tetra (Molecular Devices) at 37°C (excitation: 530 nm, emission: 560 nm). CFTR was stimulated with 10 µM forskolin (Sigma-Aldrich) and either 1 µM VX-770 (Selleck Chemicals) or DMSO. The assay was terminated with 10 µM CFTRinh172 (Cystic Fibrosis Foundation Therapeutics). Changes in membrane potential were normalized to the point before the addition of agonist and to the DMSO control response.<sup>82,83</sup>

### Protein Isolation and Western Blot Analysis

For all protein assays, total protein lysate was extracted 5 days after cellular confluency, where cells were trypsinized from their wells, pelleted, and washed three times with  $1 \times$  PBS (GIBCO). Protein was isolated by resuspension in 150 µL of a one-to-one solution of radioimmunoprecipitation assay (RIPA) homogenizing buffer (50 mM Tris HCl pH 7.4, 150 mM NaCl, 1-mM EDTA) and RIPA double-detergent buffer (2% deoxycholate, 2% NP-40, 2% Triton X-100 in RIPA homogenizing buffer) supplemented with a protease-inhibitor cocktail (Roche). Cells were subsequently incubated on ice for 30 min, then centrifuged at  $12,000 \times g$  for 15 min at 4°C. The supernatant was collected and stored at  $-80^\circ\text{C}$ . Whole protein

concentration was measured using Pierce BCA Protein Assay Kit according to the manufacturer's protocol (Thermo Fisher Scientific). SDS-PAGE separation was completed by running 10 µg of total protein on a NuPAGE 3%–8% Tris-Acetate gel (Thermo Fisher Scientific) or 6% Tris-Glycine gel (Life Technologies) as previously described.<sup>84,85</sup> Next, proteins were transferred to a nitrocellulose membrane using the iBlot 2 transfer apparatus (Thermo Fisher Scientific). A 5% milk solution in 1 × TBST was used for blocking for 1 h at room temperature. The membrane was then incubated with the CFTR primary antibody (University of North Carolina Chapel Hill: Anti-CFTR 596) at 4°C overnight. Primary antibody solution was removed, and the membrane was washed three times with 1 × TBST. This was followed by a 1-h incubation at room temperature with horseradish peroxidase conjugated goat anti-rabbit immunoglobulin G (IgG; Abcam: ab6721). For protein measurements after functional analysis, CNX was used as a loading control (Sigma: C4731). For all other protein measurements, beta-actin (ACTB) was used as a loading control (Santa Cruz: SC-47778). After three washes with 1 × TBST, signal detection was achieved using SuperSignal West Femto Maximum Sensitivity Substrate (Thermo Fisher Scientific) according to the manufacturer's protocol or with ECL (Amersham) using the Li-Cor Odyssey Fc (LI-COR Biosciences, Lincoln, NE, USA) in a linear range of exposure (2–5 min).<sup>86</sup> Relative levels of CFTR protein were quantitated by densitometry of immunoblots using ImageStudioLite (LI-COR Biosciences, Lincoln, NE, USA).<sup>87</sup>

### RNA Isolation and Quantitative PCR

Assays of *CFTR* mRNA expression were performed 5 days after cellular confluency. Cells were harvested, washed three times with 1 × PBS, and pelleted, then total RNA was extracted using the RNeasy Mini Kit following the manufacturer's protocol (QIAGEN). Next, 1,000 ng of mRNA was reverse transcribed using SuperScript III Reverse Transcriptase (Thermo Fisher Scientific) following the manufacturer's protocol. Quantitative PCR utilizing Fast SYBR Green Master Mix (QIAGEN) was performed on a Step One Plus Real Time PCR machine (Applied Biosystems). Primers specific to endogenous GAPDH were used as an internal control. Differential expression between edited and unedited samples was analyzed using the  $\Delta\Delta C_t$  method.

### Statistical Analyses

All graphs were plotted as the mean, with error bars indicating standard deviation or the standard error of the mean. Differences between groups were assessed by two-tailed unpaired t test with Welch's correction. p values less than 0.05 were considered statistically significant.

### SUPPLEMENTAL INFORMATION

Supplemental Information can be found online at <https://doi.org/10.1016/j.omtm.2020.05.002>.

### AUTHOR CONTRIBUTIONS

S.E., O.L., C.E.B., and E.A.I. conceptualized this research and designed the experiments. S.E., O.L., T.M.I.B., R.A.B., and A.H.R. per-

formed the experiments. S.E. and O.L. analyzed experimental results. S.E. and O.L. wrote the manuscript. S.E., O.L., C.E.B., and E.A.I. edited the final manuscript. All authors approved the final manuscript.

### CONFLICTS OF INTEREST

The authors declare no competing interests.

### ACKNOWLEDGMENTS

We would like to thank Kyle Lindsay and Brandon James McMurray for their technical assistance. This work was supported by The Hospital for Sick Children (Restrcomp to S.E.) and by grants to C.E.B. from Cystic Fibrosis Canada (CFC#3172) and from the Canadian Institutes of Health Research (CIHR MOP-125855).

### REFERENCES

- Mort, M., Ivanov, D., Cooper, D.N., and Chuzhanova, N.A. (2008). A meta-analysis of nonsense mutations causing human genetic disease. *Hum. Mutat.* 29, 1037–1047.
- Khajavi, M., Inoue, K., and Lupski, J.R. (2006). Nonsense-mediated mRNA decay modulates clinical outcome of genetic disease. *Eur. J. Hum. Genet.* 14, 1074–1081.
- Kerr, T.P., Sewry, C.A., Robb, S.A., and Roberts, R.G. (2001). Long mutant dystrophins and variable phenotypes: evasion of nonsense-mediated decay? *Hum. Genet.* 109, 402–407.
- Li, A., and Swift, M. (2000). Mutations at the ataxia-telangiectasia locus and clinical phenotypes of A-T patients. *Am. J. Med. Genet.* 92, 170–177.
- Kienzler, A.K., van Schouwenburg, P.A., Taylor, J., Marwah, I., Sharma, R.U., Noakes, C., Thomson, K., Sadler, R., Segal, S., Ferry, B., et al. (2016). Hypomorphic function and somatic reversion of DOCK8 cause combined immunodeficiency without hyper-IgE. *Clin. Immunol.* 163, 17–21.
- Riordan, J.R., Rommens, J.M., Kerem, B., Alon, N., Rozmahel, R., Grzelczak, Z., Zielenski, J., Lok, S., Plavsic, N., Chou, J.L., et al. (1989). Identification of the cystic fibrosis gene: cloning and characterization of complementary DNA. *Science* 245, 1066–1073.
- Bear, C.E., Li, C.H., Kartner, N., Bridges, R.J., Jensen, T.J., Ramjeesingh, M., and Riordan, J.R. (1992). Purification and functional reconstitution of the cystic fibrosis transmembrane conductance regulator (CFTR). *Cell* 68, 809–818.
- Rowe, S.M., Miller, S., and Sorscher, E.J. (2005). Cystic fibrosis. *N. Engl. J. Med.* 352, 1992–2001.
- Keating, D., Marigowda, G., Burr, L., Daines, C., Mall, M.A., McKone, E.F., Ramsey, B.W., Rowe, S.M., Sass, L.A., Tullis, E., et al.; VX16-445-001 Study Group (2018). VX-445-Tezacaftor-Ivacaftor in Patients with Cystic Fibrosis and One or Two Phe508del Alleles. *N. Engl. J. Med.* 379, 1612–1620.
- Hoy, S.M. (2019). Elexacaftor/Ivacaftor/Tezacaftor: First Approval. *Drugs* 79, 2001–2007.
- Middleton, P.G., Mall, M.A., Dřevínek, P., Lands, L.C., McKone, E.F., Polineni, D., Ramsey, B.W., Taylor-Cousar, J.L., Tullis, E., Vermeulen, F., et al.; VX17-445-102 Study Group (2019). Elexacaftor-Tezacaftor-Ivacaftor for Cystic Fibrosis with a Single Phe508del Allele. *N. Engl. J. Med.* 381, 1809–1819.
- Guerra, L., Favia, M., Di Gioia, S., Laselva, O., Bisogno, A., Casavola, V., Colombo, C., and Conese, M. (2020). The preclinical discovery and development of the combination of ivacaftor + tezacaftor used to treat cystic fibrosis. *Expert Opin. Drug Discov.* April 15, 2020. <https://doi.org/10.1080/17460441.2020.1750592>.
- Linde, L., Boelz, S., Nissim-Rafinia, M., Oren, Y.S., Wilschanski, M., Yaacov, Y., Virgilis, D., Neu-Yilik, G., Kulozik, A.E., Kerem, E., and Kerem, B. (2007). Nonsense-mediated mRNA decay affects nonsense transcript levels and governs response of cystic fibrosis patients to gentamicin. *J. Clin. Invest.* 117, 683–692.
- Aksit, M.A., Bowling, A.D., Evans, T.A., Joynt, A.T., Osorio, D., Patel, S., West, N., Merlo, C., Sosnay, P.R., Cutting, G.R., and Sharma, N. (2019). Decreased mRNA and protein stability of W1282X limits response to modulator therapy. *J. Cyst. Fibros.* 18, 606–613.

15. Haggie, P.M., Phuan, P.W., Tan, J.A., Xu, H., Avramescu, R.G., Perdomo, D., Zlock, L., Nielson, D.W., Finkbeiner, W.E., Lukacs, G.L., and Verkman, A.S. (2017). Correctors and Potentiators Rescue Function of the Truncated W1282X-Cystic Fibrosis Transmembrane Regulator (CFTR) Translation Product. *J. Biol. Chem.* *292*, 771–785.
16. Laselva, O., Eckford, P.D., Bartlett, C., Ouyang, H., Gunawardena, T.N., Gonska, T., Moraes, T.J., and Bear, C.E. (2019). Functional rescue of c.3846G > A (W1282X) in patient-derived nasal cultures achieved by inhibition of nonsense mediated decay and protein modulators with complementary mechanisms of action. *J. Cyst. Fibros.* Published online December 9, 2019. <https://doi.org/10.1016/j.jcf.2019.12.001>.
17. Mendell, J.T., Sharifi, N.A., Meyers, J.L., Martinez-Murillo, F., and Dietz, H.C. (2004). Nonsense surveillance regulates expression of diverse classes of mammalian transcripts and mutes genomic noise. *Nat. Genet.* *36*, 1073–1078.
18. He, F., Li, X., Spatrick, P., Casillo, R., Dong, S., and Jacobson, A. (2003). Genome-wide analysis of mRNAs regulated by the nonsense-mediated and 5' to 3' mRNA decay pathways in yeast. *Mol. Cell* *12*, 1439–1452.
19. Neu-Yilik, G., Gehring, N.H., Hentze, M.W., and Kulozik, A.E. (2004). Nonsense-mediated mRNA decay: from vacuum cleaner to Swiss army knife. *Genome Biol.* *5*, 218.
20. Reichenbach, P., Höss, M., Azzalin, C.M., Nabholz, M., Bucher, P., and Lingner, J. (2003). A human homolog of yeast Est1 associates with telomerase and uncaps chromosome ends when overexpressed. *Curr. Biol.* *13*, 568–574.
21. Frischmeyer, P.A., and Dietz, H.C. (1999). Nonsense-mediated mRNA decay in health and disease. *Hum. Mol. Genet.* *8*, 1893–1900.
22. Li, S., and Wilkinson, M.F. (1998). Nonsense surveillance in lymphocytes? *Immunity* *8*, 135–141.
23. Wagner, E., and Lykke-Andersen, J. (2002). mRNA surveillance: the perfect persist. *J. Cell Sci.* *115*, 3033–3038.
24. McNeer, N.A., Anandalingam, K., Fields, R.J., Caputo, C., Kopic, S., Gupta, A., Quijano, E., Polikoff, L., Kong, Y., Bahal, R., et al. (2015). Nanoparticles that deliver triplex-forming peptide nucleic acid molecules correct F508del CFTR in airway epithelium. *Nat. Commun.* *6*, 6952.
25. Vidović, D., Carlon, M.S., da Cunha, M.F., Dekkers, J.F., Hollenhorst, M.I., Bijvelds, M.J., Ramalho, A.S., Van den Haute, C., Ferrante, M., Baekelandt, V., et al. (2016). rAAV-CFTRΔR Rescues the Cystic Fibrosis Phenotype in Human Intestinal Organoids and Cystic Fibrosis Mice. *Am. J. Respir. Crit. Care Med.* *193*, 288–298.
26. Cao, H., Machuca, T.N., Yeung, J.C., Wu, J., Du, K., Duan, C., Hashimoto, K., Linacre, V., Coates, A.L., Leung, K., et al. (2013). Efficient gene delivery to pig airway epithelia and submucosal glands using helper-dependent adenoviral vectors. *Mol. Ther. Nucleic Acids* *2*, e127.
27. Cooney, A.L., Abou Alaiwa, M.H., Shah, V.S., Bouzek, D.C., Stroik, M.R., Powers, L.S., Gansemeyer, N.D., Meyerholz, D.K., Welsh, M.J., Stoltz, D.A., et al. (2016). Lentiviral-mediated phenotypic correction of cystic fibrosis pigs. *JCI Insight* *1*, 88730.
28. Steines, B., Dickey, D.D., Bergen, J., Excoffon, K.J., Weinstein, J.R., Li, X., Yan, Z., Abou Alaiwa, M.H., Shah, V.S., Bouzek, D.C., et al. (2016). CFTR gene transfer with AAV improves early cystic fibrosis pig phenotypes. *JCI Insight* *1*, e88728.
29. Cooney, A.L., McCray, P.B., Jr., and Sinn, P.L. (2018). Cystic Fibrosis Gene Therapy: Looking Back, Looking Forward. *Genes (Basel)* *9*, E538.
30. Alton, E.W., Boyd, A.C., Davies, J.C., Gill, D.R., Griesenbach, U., Harrison, P.T., Henig, N., Higgins, T., Hyde, S.C., Innes, J.A., and Korman, M.S. (2016). Genetic medicines for CF: Hype versus reality. *Pediatr. Pulmonol.* *51* (S44), S5–S17.
31. Vaidyanathan, S., Salahudeen, A.A., Sellers, Z.M., Bravo, D.T., Choi, S.S., Batish, A., Le, W., Baik, R., de la, O.S., Kaushik, M.P., et al. (2019). High-Efficiency, Selection-free Gene Repair in Airway Stem Cells from Cystic Fibrosis Patients Rescues CFTR Function in Differentiated Epithelia. *Cell Stem Cell* *26*, 161–171.
32. Schwank, G., Koo, B.K., Sasselli, V., Dekkers, J.F., Heo, I., Demircan, T., Sasaki, N., Boymans, S., Cuppen, E., van der Ent, C.K., et al. (2013). Functional repair of CFTR by CRISPR/Cas9 in intestinal stem cell organoids of cystic fibrosis patients. *Cell Stem Cell* *13*, 653–658.
33. Bednarski, C., Tomczak, K., Vom Hövel, B., Weber, W.M., and Cathomen, T. (2016). Targeted Integration of a Super-Exon into the CFTR Locus Leads to Functional Correction of a Cystic Fibrosis Cell Line Model. *PLoS ONE* *11*, e0161072.
34. Sanz, D.J., Hollywood, J.A., Scallan, M.F., and Harrison, P.T. (2017). Cas9/gRNA targeted excision of cystic fibrosis-causing deep-intronic splicing mutations restores normal splicing of CFTR mRNA. *PLoS ONE* *12*, e0184009.
35. Maule, G., Casini, A., Montagna, C., Ramalho, A.S., De Boeck, K., Debyser, Z., Carlon, M.S., Petris, G., and Cereseto, A. (2019). Allele specific repair of splicing mutations in cystic fibrosis through AsCas12a genome editing. *Nat. Commun.* *10*, 3556.
36. Chapman, J.R., Taylor, M.R., and Boulton, S.J. (2012). Playing the end game: DNA double-strand break repair pathway choice. *Mol. Cell* *47*, 497–510.
37. Lejeune, F., and Maquat, L.E. (2005). Mechanistic links between nonsense-mediated mRNA decay and pre-mRNA splicing in mammalian cells. *Curr. Opin. Cell Biol.* *17*, 309–315.
38. Maquat, L.E. (2004). Nonsense-mediated mRNA decay: splicing, translation and mRNP dynamics. *Nat. Rev. Mol. Cell Biol.* *5*, 89–99.
39. Zheng, Q., Cai, X., Tan, M.H., Schaffert, S., Arnold, C.P., Gong, X., Chen, C.Z., and Huang, S. (2014). Precise gene deletion and replacement using the CRISPR/Cas9 system in human cells. *Biotechniques* *57*, 115–124.
40. Bauer, D.E., Conner, M.C., and Orkin, S.H. (2015). Generation of genomic deletions in mammalian cell lines via CRISPR/Cas9. *J. Vis. Exp.* *95*, e52118.
41. Zhou, J., Wang, J., Shen, B., Chen, L., Su, Y., Yang, J., Zhang, W., Tian, X., and Huang, X. (2014). Dual sgRNAs facilitate CRISPR/Cas9-mediated mouse genome targeting. *FEBS J.* *281*, 1717–1725.
42. Xiao, A., Wang, Z., Hu, Y., Wu, Y., Luo, Z., Yang, Z., Zu, Y., Li, W., Huang, P., Tong, X., et al. (2013). Chromosomal deletions and inversions mediated by TALENs and CRISPR/Cas in zebrafish. *Nucleic Acids Res.* *41*, e141.
43. Labun, K., Montague, T.G., Krause, M., Torres Cleuren, Y.N., Tjeldnes, H., and Valen, E. (2019). CHOPCHOP v3: expanding the CRISPR web toolbox beyond genome editing. *Nucleic Acids Res.* *47* (W1), W171–W174.
44. Valley, H.C., Bukis, K.M., Bell, A., Cheng, Y., Wong, E., Jordan, N.J., Allaire, N.E., Sivachenko, A., Liang, F., Bihler, H., et al. (2019). Isogenic cell models of cystic fibrosis-causing variants in natively expressing pulmonary epithelial cells. *J. Cyst. Fibros.* *18*, 476–483.
45. Rowe, S.M., Varga, K., Rab, A., Bekok, Z., Byram, K., Li, Y., Sorscher, E.J., and Clancy, J.P. (2007). Restoration of W1282X CFTR activity by enhanced expression. *Am. J. Respir. Cell Mol. Biol.* *37*, 347–356.
46. Wang, W., Hong, J.S., Rab, A., Sorscher, E.J., and Kirk, K.L. (2016). Robust Stimulation of W1282X-CFTR Channel Activity by a Combination of Allosteric Modulators. *PLoS ONE* *11*, e0152232.
47. Cong, L., Ran, F.A., Cox, D., Lin, S., Barretto, R., Habib, N., Hsu, P.D., Wu, X., Jiang, W., Marraffini, L.A., and Zhang, F. (2013). Multiplex genome engineering using CRISPR/Cas systems. *Science* *339*, 819–823.
48. Jiang, W., Bikard, D., Cox, D., Zhang, F., and Marraffini, L.A. (2013). RNA-guided editing of bacterial genomes using CRISPR-Cas systems. *Nat. Biotechnol.* *31*, 233–239.
49. Pattanayak, V., Lin, S., Guilinger, J.P., Ma, E., Doudna, J.A., and Liu, D.R. (2013). High-throughput profiling of off-target DNA cleavage reveals RNA-programmed Cas9 nuclease specificity. *Nat. Biotechnol.* *31*, 839–843.
50. Heijerman, H.G.M., McKone, E.F., Downey, D.G., Van Braeckel, E., Rowe, S.M., Tullis, E., Mall, M.A., Welter, J.J., Ramsey, B.W., McKee, C.M., et al.; VX17-445-103 Trial Group (2019). Efficacy and safety of the elxacaftor plus tezacaftor plus ivacaftor combination regimen in people with cystic fibrosis homozygous for the F508del mutation: a double-blind, randomised, phase 3 trial. *Lancet* *394*, 1940–1948.
51. Wainwright, C.E., Elborn, J.S., Ramsey, B.W., Marigowda, G., Huang, X., Cipolli, M., Colombo, C., Davies, J.C., De Boeck, K., Flume, P.A., et al.; TRAFFIC Study Group; TRANSPORT Study Group (2015). Lumacaftor-Ivacaftor in Patients with Cystic Fibrosis Homozygous for Phe508del CFTR. *N. Engl. J. Med.* *373*, 220–231.
52. Yeh, J.T., and Hwang, T.C. (2019). Positional effects of premature termination codons on the biochemical and biophysical properties of CFTR. *J. Physiol.* *598*, 517–541.
53. Keenan, M.M., Huang, L., Jordan, N.J., Wong, E., Cheng, Y., Valley, H.C., Mahiou, J., Liang, F., Bihler, H., Mense, M., et al. (2019). Nonsense-mediated RNA Decay Pathway Inhibition Restores Expression and Function of W1282X CFTR. *Am. J. Respir. Cell Mol. Biol.* *61*, 290–300.

54. Guggino, W.B., and Stanton, B.A. (2006). New insights into cystic fibrosis: molecular switches that regulate CFTR. *Nat. Rev. Mol. Cell Biol.* 7, 426–436.
55. Favia, M., Guerra, L., Fanelli, T., Cardone, R.A., Monterisi, S., Di Sole, F., Castellani, S., Chen, M., Seidler, U., Reshkin, S.J., et al. (2010). Na<sup>+</sup>/H<sup>+</sup> exchanger regulatory factor 1 overexpression-dependent increase of cytoskeleton organization is fundamental in the rescue of F508del cystic fibrosis transmembrane conductance regulator in human airway CFBE41o- cells. *Mol. Biol. Cell* 21, 73–86.
56. Arora, K., Moon, C., Zhang, W., Yarlagadda, S., Penmatsa, H., Ren, A., Sinha, C., and Naren, A.P. (2014). Stabilizing rescued surface-localized  $\delta$ F508 CFTR by potentiation of its interaction with Na<sup>(+)</sup>/H<sup>(+)</sup> exchanger regulatory factor 1. *Biochemistry* 53, 4169–4179.
57. Abbattiscianni, A.C., Favia, M., Mancini, M.T., Cardone, R.A., Guerra, L., Monterisi, S., Castellani, S., Laselva, O., Di Sole, F., Conese, M., et al. (2016). Correctors of mutant CFTR enhance subcortical cAMP-PKA signaling through modulating ezrin phosphorylation and cytoskeleton organization. *J. Cell Sci.* 129, 1128–1140.
58. Lobo, M.J., Amaral, M.D., Zaccolo, M., and Farinha, C.M. (2016). EPAC1 activation by cAMP stabilizes CFTR at the membrane by promoting its interaction with NHERF1. *J. Cell Sci.* 129, 2599–2612.
59. Bidaud-Meynard, A., Bossard, F., Schnür, A., Fukuda, R., Veit, G., Xu, H., and Lukacs, G.L. (2019). Transcytosis maintains CFTR apical polarity in the face of constitutive and mutation-induced basolateral missorting. *J. Cell Sci.* 132, jcs226886.
60. Canver, M.C., Bauer, D.E., Dass, A., Yien, Y.Y., Chung, J., Masuda, T., Maeda, T., Paw, B.H., and Orkin, S.H. (2014). Characterization of genomic deletion efficiency mediated by clustered regularly interspaced short palindromic repeats (CRISPR)/Cas9 nuclease system in mammalian cells. *J. Biol. Chem.* 289, 21312–21324.
61. Lindeboom, R.G., Supek, F., and Lehner, B. (2016). The rules and impact of nonsense-mediated mRNA decay in human cancers. *Nat. Genet.* 48, 1112–1118.
62. Hall, G.W., and Thein, S. (1994). Nonsense codon mutations in the terminal exon of the beta-globin gene are not associated with a reduction in beta-mRNA accumulation: a mechanism for the phenotype of dominant beta-thalassemia. *Blood* 83, 2031–2037.
63. Thein, S.L., Hesketh, C., Taylor, P., Temperley, I.J., Hutchinson, R.M., Old, J.M., Wood, W.G., Clegg, J.B., and Weatherall, D.J. (1990). Molecular basis for dominantly inherited inclusion body beta-thalassemia. *Proc. Natl. Acad. Sci. USA* 87, 3924–3928.
64. Miller, J.N., and Pearce, D.A. (2014). Nonsense-mediated decay in genetic disease: friend or foe? *Mutat. Res. Rev. Mutat. Res.* 762, 52–64.
65. Nagy, E., and Maquat, L.E. (1998). A rule for termination-codon position within intron-containing genes: when nonsense affects RNA abundance. *Trends Biochem. Sci.* 23, 198–199.
66. Wang, J., Gudikote, J.P., Olivares, O.R., and Wilkinson, M.F. (2002). Boundary-independent polar nonsense-mediated decay. *EMBO Rep.* 3, 274–279.
67. Bühler, M., Steiner, S., Mohn, F., Paillusson, A., and Mühlemann, O. (2006). EJc-independent degradation of nonsense immunoglobulin-mu mRNA depends on 3' UTR length. *Nat. Struct. Mol. Biol.* 13, 462–464.
68. Chan, D., Weng, Y.M., Graham, H.K., Silence, D.O., and Bateman, J.F. (1998). A nonsense mutation in the carboxyl-terminal domain of type X collagen causes haploinsufficiency in Schmid metaphyseal chondrodysplasia. *J. Clin. Invest.* 101, 1490–1499.
69. Asselta, R., Duga, S., Spena, S., Santagostino, E., Peyvandi, F., Piseddu, G., Targhetta, R., Malcovati, M., Mannucci, P.M., and Tenchini, M.L. (2001). Congenital afibrinogenemia: mutations leading to premature termination codons in fibrinogen A alpha-chain gene are not associated with the decay of the mutant mRNAs. *Blood* 98, 3685–3692.
70. Rajavel, K.S., and Neufeld, E.F. (2001). Nonsense-mediated decay of human HEXA mRNA. *Mol. Cell. Biol.* 21, 5512–5519.
71. Amoasii, L., Long, C., Li, H., Mireault, A.A., Shelton, J.M., Sanchez-Ortiz, E., McAnally, J.R., Bhattacharyya, S., Schmidt, F., Grimm, D., et al. (2017). Single-cut genome editing restores dystrophin expression in a new mouse model of muscular dystrophy. *Sci. Transl. Med.* 9, eaan8081.
72. Lau, C.H., and Suh, Y. (2017). *In vivo* genome editing in animals using AAV-CRISPR system: applications to translational research of human disease. *F1000Res.* 6, 2153.
73. Wu, Z., Yang, H., and Colosi, P. (2010). Effect of genome size on AAV vector packaging. *Mol. Ther.* 18, 80–86.
74. Chew, W.L., Tabebordbar, M., Cheng, J.K., Mali, P., Wu, E.Y., Ng, A.H., Zhu, K., Wagers, A.J., and Church, G.M. (2016). A multifunctional AAV-CRISPR-Cas9 and its host response. *Nat. Methods* 13, 868–874.
75. Truong, D.J., Kühner, K., Kühn, R., Werfel, S., Engelhardt, S., Wurst, W., and Ortiz, O. (2015). Development of an intein-mediated split-Cas9 system for gene therapy. *Nucleic Acids Res.* 43, 6450–6458.
76. Zetsche, B., Volz, S.E., and Zhang, F. (2015). A split-Cas9 architecture for inducible genome editing and transcription modulation. *Nat. Biotechnol.* 33, 139–142.
77. Agudelo, D., Carter, S., Velimirovic, M., Durringer, A., Rivest, J.F., Levesque, S., Loehr, J., Mouchiroud, M., Cyr, D., Waters, P.J., et al. (2020). Versatile and robust genome editing with *Streptococcus thermophilus* CRISPR1-Cas9. *Genome Res.* 30, 107–117.
78. Kim, E., Koo, T., Park, S.W., Kim, D., Kim, K., Cho, H.Y., Song, D.W., Lee, K.J., Jung, M.H., Kim, S., et al. (2017). *In vivo* genome editing with a small Cas9 orthologue derived from *Campylobacter jejuni*. *Nat. Commun.* 8, 14500.
79. Ran, F.A., Cong, L., Yan, W.X., Scott, D.A., Gootenberg, J.S., Kriz, A.J., Zetsche, B., Shalem, O., Wu, X., Makarova, K.S., et al. (2015). *In vivo* genome editing using *Staphylococcus aureus* Cas9. *Nature* 520, 186–191.
80. Nguyen, A.D., Nguyen, T.A., Zhang, J., Devireddy, S., Zhou, P., Karydas, A.M., Xu, X., Miller, B.L., Rigo, F., Ferguson, S.M., et al. (2018). Murine knockin model for progranulin-deficient frontotemporal dementia with nonsense-mediated mRNA decay. *Proc. Natl. Acad. Sci. USA* 115, E2849–E2858.
81. Hsiau, T., Conant, D., Rossi, N., Maures, T., Waite, K., Yang, J., Joshi, S., Kelso, R., Holden, K., Enzmann, B.L., et al. (2019). Inference of CRISPR Edits from Sanger Trace Data. *bioRxiv*. <https://doi.org/10.1101/251082>.
82. Wu, Y.S., Jiang, J., Ahmadi, S., Lew, A., Laselva, O., Xia, S., Bartlett, C., Ip, W., Wellhauser, L., Ouyang, H., et al. (2019). ORKAMBI-Mediated Rescue of Mucociliary Clearance in Cystic Fibrosis Primary Respiratory Cultures Is Enhanced by Arginine Uptake, Arginase Inhibition, and Promotion of Nitric Oxide Signaling to the Cystic Fibrosis Transmembrane Conductance Regulator Channel. *Mol. Pharmacol.* 96, 515–525.
83. Laselva, O., Stone, T.A., Bear, C.E., and Deber, C.M. (2020). Anti-Infectives Restore ORKAMBI® Rescue of F508del-CFTR Function in Human Bronchial Epithelial Cells Infected with Clinical Strains of *P. aeruginosa*. *Biomolecules* 10, E334.
84. Molinski, S.V., Shahani, V.M., Subramanian, A.S., MacKinnon, S.S., Woollard, G., Laforet, M., Laselva, O., Morayniss, L.D., Bear, C.E., and Windemuth, A. (2018). Comprehensive mapping of cystic fibrosis mutations to CFTR protein identifies mutation clusters and molecular docking predicts corrector binding site. *Proteins* 86, 833–843.
85. Laselva, O., Molinski, S., Casavola, V., and Bear, C.E. (2016). The investigational Cystic Fibrosis drug Trimethylangelicin directly modulates CFTR by stabilizing the first membrane-spanning domain. *Biochem. Pharmacol.* 119, 85–92.
86. Laselva, O., Marzaro, G., Vaccarin, C., Lampronti, I., Tamanini, A., Lippi, G., Gambari, R., Cabrini, G., Bear, C.E., Chilin, A., and Dececchi, M.C. (2018). Molecular Mechanism of Action of Trimethylangelicin Derivatives as CFTR Modulators. *Front. Pharmacol.* 9, 719.
87. Chin, S., Ramjeesingh, M., Hung, M., Ereño-Oreba, J., Cui, H., Laselva, O., Julien, J.P., and Bear, C.E. (2019). Cholesterol Interaction Directly Enhances Intrinsic Activity of the Cystic Fibrosis Transmembrane Conductance Regulator (CFTR). *Cells* 8, E804.